

行政院國家科學委員會專題研究計畫 期末報告

單一量子點之磁光與糾纏態特性(2/2)

計畫類別：個別型
計畫編號：NSC 100-2628-E-009-009-
執行期間：100年08月01日至101年08月31日
執行單位：國立交通大學電子工程學系及電子研究所

計畫主持人：林聖迪

計畫參與人員：碩士班研究生-兼任助理人員：翁思強
碩士班研究生-兼任助理人員：張胤傑
博士班研究生-兼任助理人員：傅英哲
博士班研究生-兼任助理人員：李依珊

報告附件：出席國際會議研究心得報告及發表論文

公開資訊：本計畫可公開查詢

中華民國 101 年 10 月 26 日

中文摘要： 在此為期兩年的計畫中，我們進行光激發自組式量子點的發光特性之相關研究。第一部分為單一量子點發光頻譜與磁場的響應，第二部分為單一量子點與共振腔的光子-激子交互作用。基於磁場響應實驗上觀察到 negative trion 的異常 diamagnetic shift，以及其不同於傳統反磁性的順磁性行為，因此我們發展了一套 Hartree- approximation 的計算方法來模擬量子點內不同 exciton complexes 的發光行為，模擬結果顯示出與實驗結果相當一致，並且成功的定性解釋了這種異常行為，我們發現載子間的庫倫交互作用對磁場的響應跟量子點尺寸大小有相當大的關係，且此種異常行為即為載子間庫倫作用所主導。量子點與共振腔交互作用的部分，透過製作高品質因子的微柱形共振腔，我們觀察到量子點的發光特性的確受到共振效應的影響，不僅發光強度明顯變強，其偏振態也受到改變，目前正在進行數據整理與理論分析。

中文關鍵詞： 量子點, 光激螢光, 磁場, 共振腔, 偏極化

英文摘要： In this two-year project, we have studied the photoluminescence (PL) characteristics of self-assembled quantum dots (QDs). The first part is about the magnetic response and PL of single QD. Based on previously observed anomalous diamagnetic shift of negative trions and its unusual paramagnetic behavior, we develop a theoretical method using Hartree approximation to calculate the emission properties of various exciton complexes. The simulation results are consistent with the experimental ones so we can successfully explain the anomalous behavior. We find that the coulomb interaction between carriers and its response to applied magnetic field is highly related to the size of the QDs. The unusual response is dominated by the coulomb interaction between carriers. In the part of cavity-QD interaction, we have successfully fabricated a high-quality μ -pillar with embedded single QD. The enhanced emission of QD is clearly observed and, more interestingly, the polarization of emitted light is also tuned by the resonant condition. The detailed data analysis and theoretical work are undertaking.

英文關鍵詞： quantum dot, photoluminescence, magnetic field,

cavity, polarization

單一量子點之磁光與糾纏態特性

計畫編號：NSC 99-2628-E-009-092

執行期間：99年 08月 01日至101年 7月 31日

主持人：林聖迪

摘要

在此為期兩年的計畫中，我們進行光激發自組式量子點的發光特性之相關研究。第一部分為單一量子點發光頻譜與磁場的響應，第二部分為單一量子點與共振腔的光子-激子交互作用。基於磁場響應實驗上觀察到 negative trion X^- 的異常 diamagnetic shift，以及其不同於傳統反磁性的順磁性行為，因此我們發展了一套 Hartree-approximation 的計算方法來模擬量子點內不同 exciton complexes 的發光行為，模擬結果顯示出與實驗結果相當一致，並且成功的定性解釋了這種異常行為，我們發現載子間的庫倫交互作用對磁場的響應跟量子點尺寸大小有相當大的關係，且此種異常行為即為載子間庫倫作用所主導。量子點與共振腔交互作用的部分，透過製作高品質因子的微柱形共振腔，我們觀察到量子點的發光特性的確受到共振效應的影響，不僅發光強度明顯變強，其偏振態也受到改變，目前正在進行數據整理與理論分析。

Abstract

In this two-year project, we have studied the photoluminescence (PL) characteristics of self-assembled quantum dots (QDs). The first part

is about the magnetic response and PL of single QD. Based on previously observed anomalous diamagnetic shift of negative trions and its unusual paramagnetic behavior, we develop a theoretical method using Hartree approximation to calculate the emission properties of various exciton complexes. The simulation results are consistent with the experimental ones so we can successfully explain the anomalous behavior. We find that the coulomb interaction between carriers and its response to applied magnetic field is highly related to the size of the QDs. The unusual response is dominated by the coulomb interaction between carriers. In the part of cavity-QD interaction, we have successfully fabricated a high-quality μ -pillar with embedded single QD. The enhanced emission of QD is clearly observed and, more interestingly, the polarization of emitted light is also tuned by the resonant condition. The detailed data analysis and theoretical work are undertaking.

Methods and results

Part I. Magnetic response of PL from QDs

The InAs QDs were grown on GaAs (100) substrate using the Stranski-Krastanow mode by a

Varian Gen II molecular beam epitaxy system. The InAs QDs were grown without substrate rotations, yielding a gradient in area dot density ranging from 10^8 to 10^{10} cm^{-2} . To isolate individual QDs, a 100-nm-thick aluminum metal mask was fabricated on the sample surface with arrays of 0.3- μm apertures using electron-beam lithography. Single QD spectroscopies were carried out at 5-8 K in a specially designed $\mu\text{-PL}$ setup, where the sample was mounted in a low-temperature stage and inserted in the bore of 6-T superconducting magnet for magneto-PL measurement. A He-Ne laser beam was focused onto the aperture through a microscope objective (N. A. = 0.5). The PL signals were collected by the same objective, analyzed by a 0.75-m grating monochromator, and detected by a liquid-nitrogen-cooled CCD camera, which yield a resolution limited spectral linewidth of about 60 μeV . Several apertures containing only one QD have been investigated and all of which showed similar spectral features, which in general consist of four emission lines associated with the recombination of neutral excitons (X), biexcitons (XX), positive and negative trions (X^+ and X^-).

Magneto-PL measurements have been performed on a total of seven QDs with X energy distributed over the range of 1349-1385 meV. Representative spectra selected from one particular dot (QD1) are shown in Fig. 1. When a magnetic field B was applied along the QD growth direction (Faraday geometry), each line splits into a doublet through the Zeeman effect. As

shown in Fig. 1(b), the average energy of each Zeeman doublet increases with the increasing B , known as the diamagnetic shift.

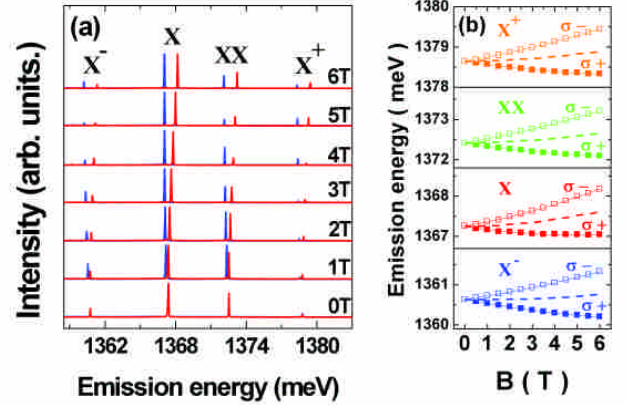


Fig. 1: (a) The magneto-PL spectra for QD1 under a magnetic field $B = 0-6$ T. (b) The corresponding peak energies of different excitonic species as a function of B for QD1, where σ^- and σ^+ in each form a Zeeman doublet. Dash line is the average energy of σ^- and σ^+ .

In Fig. 2, the measured diamagnetic shifts for the four excitonic emission lines are plotted as a function of B^2 . For X , X^+ and XX , the measured diamagnetic shifts show a quadratic dependence $\Delta E = \gamma B^2$, with a clear trend of $\gamma_X > \gamma_{XX} \cong \gamma_{X^+}$. This trend holds for all investigated dots and is a consequence of different magnetic responses of inter-particle Coulomb energies. In very strong contrast, the diamagnetic shift for the X^- does not follow the quadratic dependence. If we still use a quadratic dependence to fit the anomalous diamagnetic shift, the diamagnetic coefficient γ_{X^-} was found to be the smallest one among the four excitonic species, as depicted in Fig. 3.

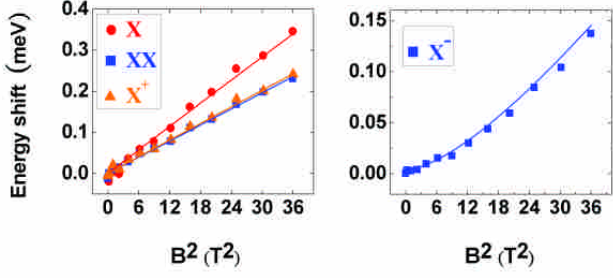


Fig. 2: Emission energy of exciton complexes shift with B^2 for QD1. The simulated QD is of 11.6 nm in diameter and 1.1 nm in height. Points are the measured data and lines are the simulated result.

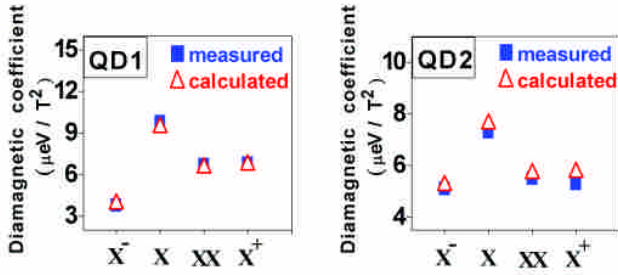


Fig. 3: The diamagnetic coefficient of the exciton complexes for the two typical QDs (QD1 and QD2). The simulated parameters are diameter of 11.6 nm and height of 1.1 nm (QD1); diameter of 11 nm and height of 1.4 nm (QD2).

The reduced optical diamagnetic coefficient of X^- could be caused either by relatively localized particle wave functions of the initial X^- state or extended electron wave function in the final $1e$ state. In the latter, the electron wave function is free of inter-particle interactions and determined solely by the confining potential of QD. By contrast, a particle in a few-particle X^- complex is subjected to additional inter-particle (e-e and e-h) interactions. The extents of the particle wave functions of the X^- and $1e$ states could become substantially different if the inter-particle interactions are comparable to or even stronger than the confining strength of QD. The hole wave functions are much more localized

than those of electrons in such small QDs. The imbalanced e-h and e-e interactions yield a net Coulomb attraction to electrons in X^- and thus make the extent of the electron wave function of the X^- state smaller than that of $1e$ state. To confirm such a scenario for the explanation of the observed anomalous diamagnetic behavior, we perform the numerical simulation for the wave functions of interacting particles in X complexes, implemented by using the finite element method within the Hartree approximation.

In the Hartree approximation, the Schrodinger equation of a particle in an interacting X complex confined in QD is written as

$$\left[H_{sp}(\vec{r}_i) + V_H(\vec{r}_i) \right] \varphi_n(\vec{r}_i) = \varepsilon_n^i \varphi_n(\vec{r}_i) \quad (1)$$

where \vec{r}_i denotes the position coordinate of the i -th particle, $H_{sp}(\vec{r}_i)$ stands for the Hamiltonian of the (non-interaction) electron or hole, ε_n^i the eigenenergy, $\varphi_n(\vec{r}_i)$ the particle wave function of the eigenstate $|n\rangle$, and $V_H(\vec{r}_i)$ is the Hartree potential, a sum of the electrostatic potentials induced by other charged particles besides the considered particle itself.

In the calculation, cone-shaped QDs of various sizes sitting on a 0.4-nm-thick wetting layer are considered. For an N -particle X complex, the N -coupled equations for each particle according to Equation (1) are self-consistently solved by using iterative approach. The total

energy of the N-particle X complex is then determined by the sum of single particle energies $\{\varepsilon^i\}$ but subtracted by the doubly counted inter-particle interaction energy. The simulated results of diamagnetic coefficients for four different exciton complexes are plotted in Fig. 4. The diamagnetic coefficients are obtained by taking the second derivative of magneto-energy spectra with respect to B using three-point numerical differentiation.

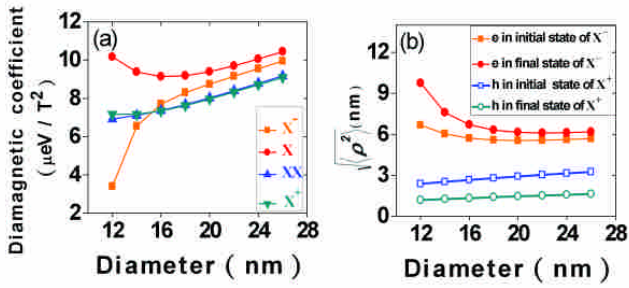


Fig. 4: The simulation for QDs with various diameters, the diamagnetic coefficients (a), and the mean radiuses of electron and hole wavefunctions in their initial and final states (b).

We first discuss the QD's size effect on the diamagnetic shifts. The calculated diamagnetic coefficients for the four exciton complexes in QDs with a diameter ranging from 12 to 26 nm are shown in Fig. 4(a). For large-sized QDs ($D > 16\text{nm}$), the diamagnetic coefficients of the four exciton complexes show similar increasing trends with the QD size. Because the diamagnetic coefficient is proportional to the area of carrier's wave function, which will reflect the dot diameter for large-size QDs. However, for smaller QD sizes ($D < 16\text{nm}$), the calculated values of γ_X increase with the

decreasing dot size, while those of γ_{XX} and γ_{X^+} remain nearly unchanged. The most striking feature is that the calculated γ_{X^-} drops rapidly with the decreasing dot size. It is worth to mention that our self-consistent calculations reproduce the experimental finding of $\gamma_X > \gamma_{XX} \cong \gamma_{X^+}$ very well, in consist with pervious calculations based on configuration-interaction methods.

For the emission of negative trion X^- , the initial state consists of two electrons and one hole, leaving one electron in its final state after recombination. The X^- diamagnetic shift thus reflects the diamagnetic responses of both the initial and final states. To understand the anomalous behavior for the X^- , it is necessary to take a closer look at the lateral extent $\ell_e \equiv \sqrt{\langle \rho_e^2 \rangle}$ of the electron wave functions before and after photon emission. Fig. 4(b) shows the calculated wave function extents $\ell_{e,i}$ and $\ell_{e,f}$ for the initial-state and the final-state electrons of X^- , respectively. One can see that the $\ell_{e,f}$ is always more or less larger than $\ell_{e,i}$. This can be realized from the presence of hole in its initial state, which contracts the electron wave function by the Coulomb attraction. When the sizes of QDs are larger than about 16nm, the differences between $\ell_{e,i}$ and $\ell_{e,f}$ are small, i.e., the presence of hole doesn't change the electron wave function significantly. However, as the QD sizes reduce, $\ell_{e,f}$ increases rapidly, with a rate even faster than $\ell_{e,i}$. Such an increasing trend for $\ell_{e,f}$ indicates

that the electron gradually loses confinement as the dot size reduces, which pushes the electron level toward the wetting-layer continuum, resulting in a very extended electron wave function penetrating into the barrier material. In such a case of weak confinement regimes, the very extended initial-state electron becomes sensitive to the long-range Coulomb attractive potential produced by the hole, by which $\ell_{e,i}$ will be contracted and become apparently smaller than $\ell_{e,f}$. As a result, the final-state diamagnetic shift increases, so that the overall diamagnetic shift in X^- is reduced. This explains why the X^- diamagnetic shift decreases rapidly for small-sized QDs shown in Fig. 4(a).

Likewise, for the emission of positive trion X^+ , the initial state consists of one electron and two holes, leaving one hole in its final state after recombination. As shown in Fig. 4(b), unlike X^- , the lateral extents of hole wave functions $\ell_h \equiv \sqrt{\langle \rho_h^2 \rangle}$ in the initial and final states are almost identical for all QD sizes. Due to the larger effective mass of holes, their wave functions are well confined even in such small QDs. In this case, the Coulomb attractive potential produced by the weakly confined electron becomes less important, so that the size dependence of γ_{X^+} behaves as usual.

Now one may ask the question why the X^- diamagnetic shift exhibits a non-quadratic B dependence. In general, a quadratic diamagnetic shift holds only in the weak-field limit, i.e., when

the magnetic length $\ell_M = \sqrt{\hbar/eB}$ is large compared to the lateral extents of carrier's wave functions $\ell = \sqrt{\langle \rho^2 \rangle}$. We noted that $\ell_M = 15$ nm at $B = 3$ T, which becomes comparable with $\ell_{e,f} = 10$ nm for the final-state electron in a QD with a base diameter of 12 nm. In this regime, the diamagnetic shift would deviate from the typical B^2 dependence. To illustrate this behavior, we consider the diamagnetic shift in the carrier's single-particle energy and expand it in powers of B as, $\Delta\varepsilon_\alpha^{SP}(B) = \gamma_\alpha B^2 + \kappa_\alpha B^4 + \dots$, where the quadratic and quartic coefficients are $\gamma_\alpha = e^2 \ell_\alpha^2 / 8m_\alpha$ and $\kappa_\alpha = -e^4 \ell_\alpha^6 / 128m_\alpha \hbar^2$, in which $\alpha = e$ or h denotes electron or hole, and m_α represents the effective mass of the electron or hole. Because $|\kappa/\gamma|$ varies as $\sim \ell^4$, the contribution from the B^4 term becomes increasingly important as $\ell \sim \ell_M$. By taking into account the difference between $\ell_{e,i}$ and $\ell_{e,f}$, a simple algebraic analysis for the X^- diamagnetic shift $\Delta E_{X^-}(B)$ gives the following expression:

$$\Delta E_{X^-}(B) \approx \gamma_{X^-} B^2 + \kappa_{X^-} B^4 + \dots \quad (2)$$

where $\gamma_{X^-} = (2\gamma_{e,i} + \gamma_{h,i}) - \gamma_{e,f}$ and $\kappa_{X^-} = (2\kappa_{e,i} + \kappa_{h,i}) - \kappa_{e,f}$. Because of $\ell_h < \ell_e$ and $m_h \gg m_e$, the $\gamma_{h,i}$ and $\kappa_{h,i}$ for the hole only have minor influences on the overall diamagnetism. Accordingly, we obtain $\gamma_{X^-} \approx 2\gamma_{e,i} - \gamma_{e,f} = e^2(2\ell_{e,i}^2 - \ell_{e,f}^2)/8m_e$ and

$$\kappa_{X^-} \approx 2\kappa_{e,i} - \kappa_{e,f} = -e^4(2\ell_{e,i}^6 - \ell_{e,f}^6)/128m_e\hbar^2 \quad .$$

Equation (2) makes clear how the difference in $\ell_{e,i}$ and $\ell_{e,f}$ can lead to anomalous diamagnetic behaviors for the emission energy of X^- . We first consider a normal case of $\ell_{e,i} \approx \ell_{e,f} = \ell_e$, we have

$$\gamma_{X^-} \approx \gamma_e \approx \gamma_X \quad \text{and} \quad |\gamma_{X^-}| \gg |\kappa_{X^-}|, \quad \text{as long as}$$

$\ell_e < \ell_M$. That is, the X^- diamagnetic shift behaves as the usual quadratic dependence with a coefficient similar to that of X , which is just the case for large-size QDs shown in Fig. 5(a). A very

interesting case occurs when $\sqrt{2}\ell_{e,i} = \ell_{e,f}$, i.e.,

$\ell_{e,i}$ of the initial-state electrons were contracted to $\sim 70.7\%$ of its final state extension $\ell_{e,f}$ by the hole. In this special case, the condition

$$2\gamma_{e,i} = \gamma_{e,f}$$

cancels out the B^2 term, leading to a dominant quartic dependence on B . As the difference between $\ell_{e,i}$ and $\ell_{e,f}$ becomes even

larger ($\sqrt{2}\ell_{e,i} < \ell_{e,f}$), the magnetic response of

X^- goes into a new regime where the quadratic coefficient γ_{X^-} is negative, i.e. the energy shift is

paramagnetic. This anomalous behavior can be best seen from the calculated results shown in Fig. 5(a), where we keep $\ell_{e,f} = 10$ nm but varying $\ell_{e,i}$

from 7.6 to 6.6 nm. The magnetic response of X^-

emissions transitioned gradually from the usual quadratic diamagnetic shift to quartic dependences, and finally into an overall negative energy shift, resembling *paramagnetic* behaviors. In Fig. 5(b), we selected four typical QDs that could represent the behaviors in different regimes, in qualitative

agreement with our calculations.

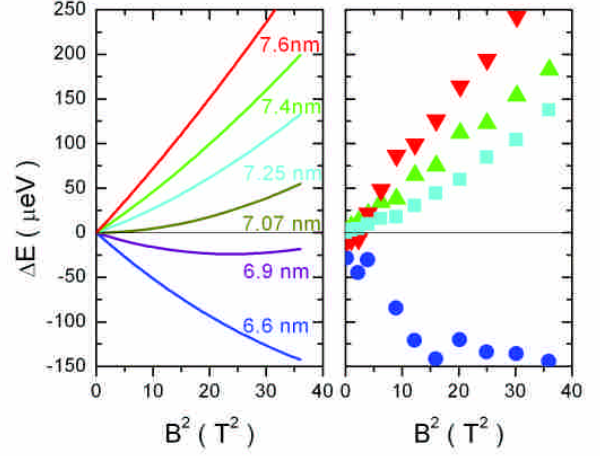


Fig. 5: The theoretical (left) and experimental (right) anomalous diamagnetic shifts in small QDs.

The magnetic responses of negative trions X^- in single self-assembled InAs/GaAs quantum dots have been investigated. Unlike the conventional quadratic diamagnetic shift for neutral excitons, the X^- diamagnetic shifts in most of the investigated dots were found to be considerably small and non-quadratic. In particular, we also observed a reversal in sign of the conventional diamagnetic shift. Theoretical analysis indicates that such anomalous behaviors for X^- arise from an apparent change in the electron wave function extent after photon emission due to the strong Coulomb attraction induced by the hole in its initial state. This effect can be very pronounced in small quantum dots, where the electron wave function becomes weakly confined and extended much into the barrier region. When the electrons gradually lose confinement, the magnetic response of X^- will transit gradually from the usual quadratic

diamagnetic shift to a quartic dependence, and finally into a special *paramagnetic* regime with an overall negative energy shift.

Part II. Cavity-QD interaction

For defining the interaction strength between cavity mode (CM) and exciton (X), temperature-varying technique was implemented on the sample since the quantum dot exciton changes more drastically with temperature than the cavity mode. For the micropillar of quality factor 6,300, the exciton was brought to resonant with cavity mode at 35.2K as Fig. 6 indicates. The energy crossing between CM and X could be observed more clearly while the peak energy was depicted as a function of temperature as shown in Fig. 7. So the pillar under investigation can be inferred to be in weak coupling regime. The PL linewidth depicted in Fig. 8 also evidences that exciton state does not couple strongly to cavity mode since the linewidth of X remains unchanged no matter detuned near or away from CM.

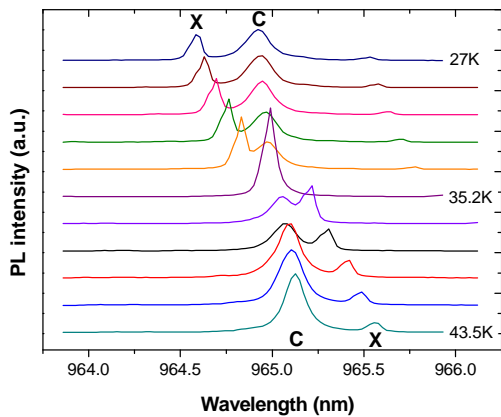


Fig. 6 Temperature-dependent PL spectrum

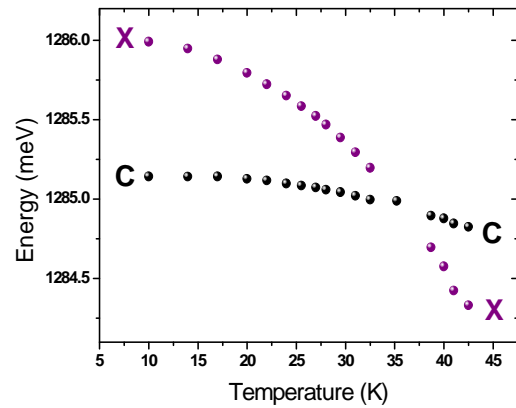


Fig. 7 PL peak energy as a function of temperature

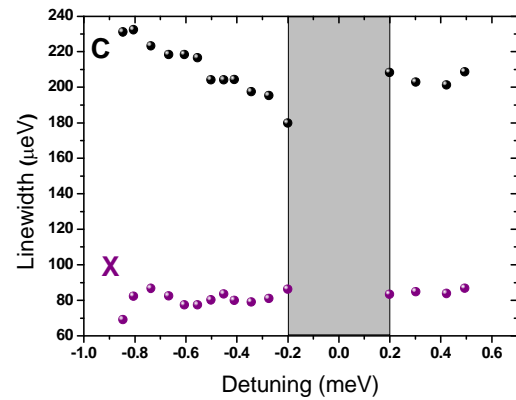


Fig. 8 PL linewidth as a function of detuning energy between CM and X

To systematically investigate the spin polarization of quantum dot exciton coupled to cavity mode, we first examine the impact of cavity on the linear polarization of exciton emission. At 10K, the exciton emission (black solid-square in Fig. 9) is polarized at 37.7° which is oriented 52° with respect to the cavity mode (red open-square in Fig. 9) as Fig. 9 presents. According to Purcell equation, the Purcell effect can be modulated as the energy detuning between X and CM is varied. Through varying temperature, the energy detuning between X and CM can be changed and thus the Purcell enhancement can be changed as well.

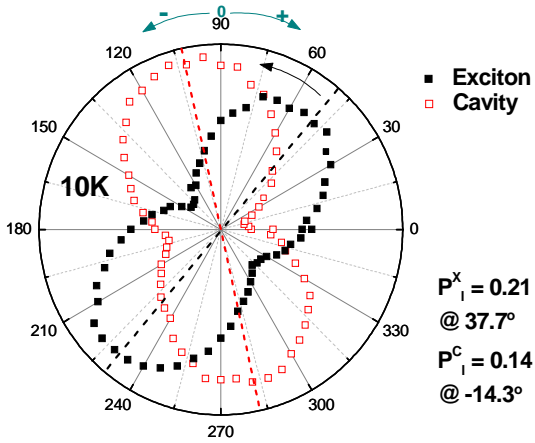


Fig. 9 Polarization plane of exciton and cavity mode at 10K for pillar A.

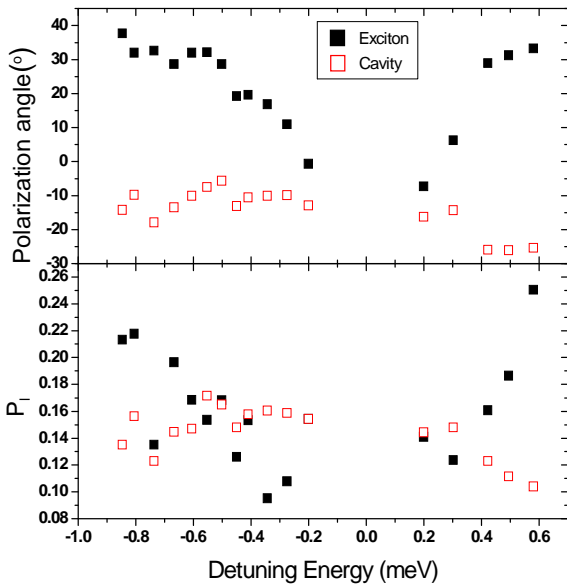


Fig. 10 Polarization angle and degree of linear polarization as a function of detuning energy for pillar A

As shown in the lower part of Fig. 10, the polarization degree decreases with negative energy detuning and increases with positive energy detuning. The linear polarization degree here is defined by $\frac{I_{\max} - I_{\min}}{I_{\max} + I_{\min}}$ since the dipole emission does not polarize along x or y axis. To one's knowledge from Purcell effect, only the polarization degree will be modified by Purcell

effect as long as X is orthogonal or parallel to CM. This modification of polarization degree is due to preferential enhancement of QD spontaneous emission rate which is caused by the difference in the quality factor between two polarized cavity modes. Though as shown in the upper part of Fig. 10 the polarization angle changes unexpectedly from 40° to 0° as energy detuning goes to zero, that is, X is detuned near CM, and relaxes to its original angle as X is detuned away from CM. As mentioned before, cavity mode modulates the emission from quantum dot as the emission dipole of X and CM is mutually orthogonal or parallel. The emission dipole of X shown in Fig. 9 is however neither parallel nor orthogonal to CM. The included angle of emission dipole between X and CM is expected to be a major factor that induces the change of polarization degree accompanying with the rotation of polarization plane.

This argument is supported and evidenced by a series of measurement implemented on pillars which appear various orientations of emission dipole between X and CM. Among pillars under investigation, pillar B has the condition that the emission dipole of X and CM is initially parallel to each other as Fig. 11 indicates. As a result, the polarization angle did not change with energy detuning but the polarization degree has a substantial increase which goes from 0.2 to 0.4 as X is detuned away from CM, which is shown in Fig. 11. The change in the polarization degree indicates that the quantum dot exciton is free of

the control of cavity mode and becomes primitive. For pillar C, as shown in Fig. 12, exciton orienting an acute angle with respect to cavity mode, the polarization plane of exciton emission thus rotates toward that of cavity mode as exciton is detuned near CM. However, the polarization degree of exciton remains unchanged as changing energy detuning and exhibits almost same quantity with that of cavity mode. The above-mentioned pillars lead to the possibility that the polarization properties of a quantum dot, which has been testified to be a single photon source, can be controlled to desired emission polarization and emit light more efficiently by interacting with cavity mode.

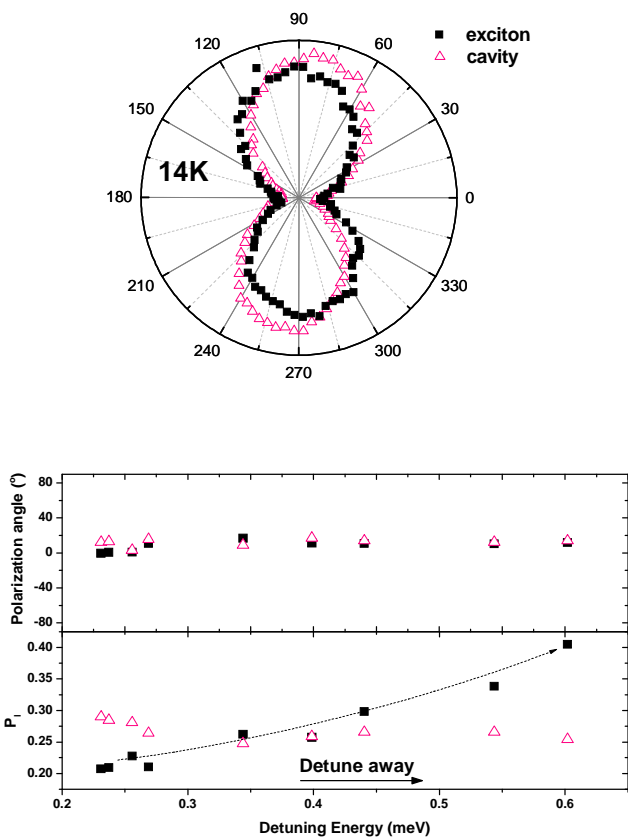


Fig. 11 The emission dipole of X and CM and the polarization angle and polarization degree as a function of energy detuning for pillar B.

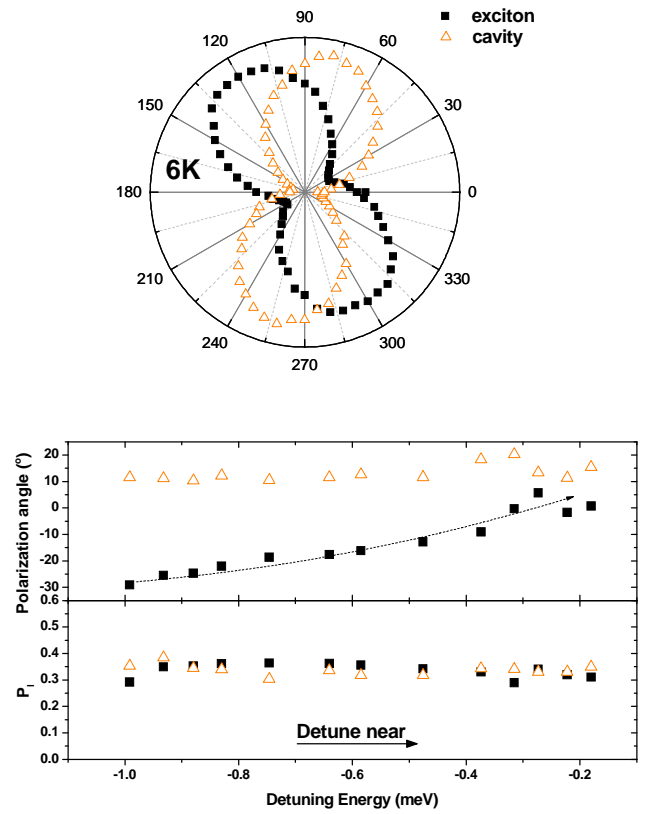


Fig. 12 The emission dipole of X and CM and the polarization angle and polarization degree as a function of energy detuning for pillar C.

In conclusion, at current stage we have not yet perform the investigation on the spin polarization state of a quantum dot while concerning the radiative lifetime modulated by a cavity mode. Nevertheless, there is still an interesting finding that Purcell effect results in a rotation of polarization plane and simultaneously a change in the polarization degree. The polarization plane of exciton seems to be clamped at the orientation of cavity mode as approaching zero detuning. This gives hint that we can precisely control the polarization orientation and degree of quantum dot exciton once the polarization pattern of cavity mode is decided.

Publications

Journal papers

1. “Lateral two-dimensional p-i-n diode in a completely undoped GaAs/AlGaAs quantum well”, V. T. Dai*, **S. D. Lin**, S. W. Lin, J. Y. Wu, L. C. Li, C. P. Lee, accepted by Jpn. J. Appl. Phys. (Oct. 2012).
2. “Superconductivity in an aluminum film grown by molecular beam epitaxy”, C.-T. Liang*, M.-R. Yeh, **S. D. Lin**, S. W. Lin, and J. Y. Wu, T. L. Lin, K. Y. Chen, Chinese J. Phys. 50, 638 (Aug. 2012).
3. “Imbalanced initial populations between dark and bright states in semiconductor quantum dots”, **S. D. Lin***, Y. J. Fu, C. Cheng, Opt. Express 20, 19850 (Aug. 2012).
4. “Observation of long-lived excitons in InAs quantum dots under thermal redistribution temperature”, C. Cheng, **S. D. Lin***, C. H. Pan, C. H. Lin, Y. J. Fu, Phys. Lett. A 376, 1495 (Mar. 2012).
5. “Selecting detection wavelength of resonant cavity-enhanced photodetector by guided-mode resonance reflector”, K. W. Lai, Y. S. Lee, Y. J. Fu, **S. D. Lin***, Opt. Express 20, 3572 (Feb. 2012).
6. “Effect of the electromagnetic environment on the dynamics of charge and phase particles in one-dimensional arrays of small Josephson junctions”, I. L. Ho, W. Kuo, **S. D. Lin**, C. P. Lee, C. T. Liang, C. S. Wu*, C. D. Chen, Euro. Phys. Lett. 96, 47004 (Nov. 2011).
7. “Stress tuning of strong and weak couplings between quantum dots and cavity modes in microdisk microcavities”, H. Lin, C. H. Lin, W. C. Lai, Y. S. Lee, **S. D. Lin**, W. H. Chang*, Phys. Rev. B 84, 201301(R) (Nov. 2011).
8. “Anomalous optical magnetic shift of self-assembled GaSb/GaAs quantum dots”, T. C. Lin*, **S. D. Lin**, L. C. Li, Y. W. Suen, C. P. Lee, J. Appl. Phys. 110, 013522 (July 2011).
9. “Anticorrelation between the splitting and polarization of the exciton fine structure in single self-assembled InAs/GaAs quantum dots”, C. H. Lin, W. T. Yu, H. Y. Chou, S. J. Cheng, **S. D. Lin**, W. H. Chang*, Phys. Rev. B 83, 075317 (Feb. 2011).
10. “A delta-doped quantum well system with additional modulation doping”, D. S. Luo, L. H. Lin, Y. C. Su, Y. T. Wang, Z. F. Peng, S. T. Lo, K. Y. Chen, Y. H. Chang, J. Y. Wu, Y. Lin, **S. D. Lin**, J. C. Chen, C. F. Huang, C.-T. Liang*, Nanoscale Res. Lett. 6, 139 (Feb. 2011).
11. “Magnetotransport in an aluminum thin film on a GaAs substrate grown by molecular beam epitaxy”, S. T. Lo, C. Chuang, **S. D. Lin***, K. Y. Chen, C.-T. Liang*, S. W. Lin, J. Y. Wu, M. R. Yeh, Nanoscale Res. Lett. 6, 102 (Feb. 2011).
12. “On the direct insulator-quantum Hall transition in two-dimensional electron systems in the vicinity of nanoscaled scatterers”, C.-T. Liang*, L.-H. Lin, K. Y. Chen, S. T. Lo, Y. T. Wang, D. S. Lou, G.-H. Kim, Y. H. Chang, Y. Ochiai, N. Aoki, J. C. Chen, Y. Lin, C. F. Huang, **S. D. Lin**, D. A. Ritchie, Nanoscale Res. Lett. 6, 131 (Feb. 2011).
13. “Electron delocalization of tensily-strained GaAs quantum dots in GaSb matrix”, T. C. Lin*, Y. H. Wu, L. C. Li, Y. T. Sung, **S. D. Lin**, L. Chang, Y. W. Suen, C. P. Lee, J. Appl. Phys. 108, 123503 (Dec. 2010).
14. “2~3 μm mid infrared light sources using InGaAs/GaAsSb "W" type quantum wells on InP substrates”, C. H. Pan*, **S. D. Lin**, C. P. Lee, J. Appl. Phys. 108, 103105 (Nov. 2010).
15. “Strong coupling of different cavity modes in photonic molecules formed by two adjacent microdisk microcavities”, H. Lin, J. H. Chen, S. S. Chao, M. C. Lo, **S. D. Lin**, W. H. Chang*, Opt. Express 18, 23948 (Nov. 2010).
16. “Wide spectral range confocal microscope based on endlessly single-mode fiber”, R. Hubbard, Yu. B. Ovchinnikov, J. Hayes, D. J. Richardson, Y. J. Fu, **S. D. Lin**, P. See, A.G. Sinclair*, Opt. Express 18, 18811 (Aug. 2010).

Conference report

1. “Cavity-modulated emission polarization of exciton in quantum-dot-embedded micro-pillar structure”, Y. S. Lee, **S. D. Lin**, International Conference on Spintronics, Sydney, Australia (July, 2012).
2. “Wavelength sensitive PIN photodetector using guided mode resonance”, K. W. Lai, **S. D. Lin**, Y. J. Fu, Y. S. Lee, Solid State

Devices and Materials (SSDM), Nagoya, Japan (Sept. 2011).

3. “Low-temperature Hump of Time-resolved Photoluminescence in InAs quantum dots”, C. Cheng, **S. D. Lin**, C. H. Pan, C. H. Lin, IEEE 2011 International Nano-Electronics Conference, Tao-Yuan, Taiwan (Jun. 2011).
4. “Room temperature 2.38 μm laser using InGaAs/GaAsSb W-type quantum wells on InP substrate”, C. H. Pan, C. H. Chang, **S. D. Lin**, C. P. Lee, Optics and Photonics Japan (OPJ 2010), Tokyo, Japan (Nov. 2010).
5. “Magneto-optical studies of GaAs quantum dots in GaSb”, T. C. Lin, **S. D. Lin**, and C P. Lee, 16th International Conference in Molecular Beam Epitaxy 2010, Berlin, German (Aug. 2010).

國科會補助專題研究計畫項下出席國際學術會議心得報告

日期：101 年 08 月 03 日

計畫編號	NSC 100-2628-E-009-009-		
計畫名稱	單一量子點之磁光與糾纏態特性(2/2)		
出國人員姓名	李依珊	服務機構及職稱	交通大學電子所博士生
會議時間	101 年 7 月 23 日 至 101 年 7 月 25 日	會議地點	澳洲雪梨
會議名稱	(中文) 世界大學網路之自旋電子學第四屆國際會議 (英文) The 4th WUN International Conference on Spintronics		
發表論文題目	(中文) 在量子點嵌於微型圓柱系統中利用共振腔調變激子發光的偏振特性 (英文) Cavity-modulated emission polarization of exciton in quantum dot-embedded micropillar structure		

一、參加會議經過

This conference was held in the new law building, University of Sydney. The committee invites two plenary speakers. One of them is Professor Hideo Ohno who plays an influential role in the field of spintronics. His researches include physics and applications of spin-related phenomena in semiconductor and in metal-based nanostructures. Another is Doctor Stuart Parkin who is an IBM Fellow. Dr. Parkin's discoveries in magneto-resistive thin film structures enable a 1000 fold increased in the storage capacity of magnetic disk drives in little more than a decade.

For the first day(7/23) of conference, following the opening ceremony there are two topics opened up in two seminar rooms which are magnetic semiconductors and spin dynamics/ transport respectively. At the beginning, Prof. Ohno gave a talk that overall reviewed the findings and phenomena of the ferromagnetism in semiconductors. After this talk, I attended the topic of spin dynamics and transport. There are two invited talks which are given by professors came from University of Sydney and institute of France respectively. Those are impressive talks that bring me into the really spin world including the control of spin coherent process in organic semiconductors and terahertz radiation from spin

excitation in magnetic semiconductors. Following the morning talk, I presented our work in the topic of spin dynamics in the afternoon. Before the end of first day, there is a poster session. Among 27 posters, what most impressed me is that Professor Tang came from China built a molecular beam epitaxy contained in-situ atoms-grown monitoring and in-chamber Raman spectrum measurement. This is really a complicated and difficult work for us who are also doing molecular beam epitaxy. The technique might help a lot in upgrading the quality of epilayers.

For the second day in the morning (7/24), I still attended the topic of spin dynamics since this topic is relatively close to the field that we are researching. What most interests me is the talk about optically-induced magnetization switching in TbFeCo thin films. The switching speed of magnetization approaches 240 femtosecond which is rather fast for operation. In the afternoon, I changed to another room for the topic of magnetic semiconductors. A simulation work has been done very well on the prediction of electronic and magnetic properties of magnetic ion doped semiconductor quantum dots by Prof. Cheng. The interplay between various relevant spin interactions and the discrete nature of Mn²⁺ spin distribution is shown in the talk to be essential in the magnetism of few Mn²⁺-doped quantum dots.

In the final day (7/25), I gained much Seebeck-knowledge from the talks with topics “Magneto-Seebeck effect in magnetic tunnel junction” and “Spin caloritronics in magnetic tunnel junction nanodevices”. Those are related to the sensing of heat. For realizing a good heat sensor, one must design a structure that can give rise to an amount of voltage or magnetic field under the application of heat gradient. The talk just presents how good the Seebeck factor is for their magnetic tunnel junction. Another talk attracted me most is the simulation of spin and charge pumping in multilayer. Prof. Chang uses an approach of nonequilibrium Green function. The work is indeed practical and gives insights for the study in the spin and carrier transfer of multilayer structure.

二、與會心得

The core of motivation for me to attend this conference is to share and to gain feedbacks from the worldwide professors. They are all professional and experienced in the field of spintronics. After I presented our work, there are one suggestion and two comments brought up by three professors. One suggests that we can apply vertical electric field to modulate the fine structure of quantum dot and then make this condition interact further with the cavity effect. It is a think-worth suggestion but have some kinds of difficulty to realize. Two professors comment that this work has an interesting finding.

There are people from over 30 countries attending this conference. Which means this conference is so grand and important hence attracts many people to attend. I am glad to be one of them since I learned very much from this meeting. I stepped into the field that I have never touched and even heard about. I gained much knowledge about the properties of various magnetic structures and organic structures those are very important in the application of quantum computers and quantum cryptology. Even though we are doing totally different works, we are still encouraged and excited through sharing the ideas with each other.

三、考察參觀活動(無是項活動者略)

四、建議

Everything is fine but just with one suggestion proposed. The expense of travel insurance should be included into the items.

五、攜回資料名稱及內容

WUN-SPIN 2012 Program and abstracts.

It contains the scientific program, introduction of plenary speakers and abstracts.

六、其他

無研發成果推廣資料

100 年度專題研究計畫研究成果彙整表

計畫主持人：林聖迪		計畫編號：100-2628-E-009-009-					
計畫名稱：單一量子點之磁光與糾纏態特性(2/2)							
成果項目		量化			單位	備註（質化說明：如數個計畫共同成果、成果列為該期刊之封面故事...等）	
		實際已達成數（被接受或已發表）	預期總達成數(含實際已達成數)	本計畫實際貢獻百分比			
國內	論文著作	期刊論文	0	0	100%	篇	
		研究報告/技術報告	0	0	100%		
		研討會論文	0	0	100%		
		專書	0	0	100%		
	專利	申請中件數	0	0	100%	件	
		已獲得件數	0	0	100%		
	技術移轉	件數	0	0	100%	件	
		權利金	0	0	100%	千元	
	參與計畫人力 (本國籍)	碩士生	2	2	100%	人次	
		博士生	2	2	100%		
博士後研究員		0	0	100%			
專任助理		0	0	100%			
國外	論文著作	期刊論文	16	18	40%	篇	
		研究報告/技術報告	0	0	100%		
		研討會論文	5	6	70%		
		專書	0	0	100%	章/本	
	專利	申請中件數	0	0	100%	件	
		已獲得件數	0	0	100%		
	技術移轉	件數	0	0	100%	件	
		權利金	0	0	100%	千元	
	參與計畫人力 (外國籍)	碩士生	0	0	100%	人次	
		博士生	0	0	100%		
博士後研究員		0	0	100%			
專任助理		0	0	100%			

<p>其他成果 (無法以量化表達之成果如辦理學術活動、獲得獎項、重要國際合作、研究成果國際影響力及其他協助產業技術發展之具體效益事項等，請以文字敘述填列。)</p>	<p>無</p>
--	----------

	成果項目	量化	名稱或內容性質簡述
科 教 處 計 畫 加 填 項 目	測驗工具(含質性與量性)	0	
	課程/模組	0	
	電腦及網路系統或工具	0	
	教材	0	
	舉辦之活動/競賽	0	
	研討會/工作坊	0	
	電子報、網站	0	
	計畫成果推廣之參與(閱聽)人數	0	

國科會補助專題研究計畫成果報告自評表

請就研究內容與原計畫相符程度、達成預期目標情況、研究成果之學術或應用價值（簡要敘述成果所代表之意義、價值、影響或進一步發展之可能性）、是否適合在學術期刊發表或申請專利、主要發現或其他有關價值等，作一綜合評估。

1. 請就研究內容與原計畫相符程度、達成預期目標情況作一綜合評估

達成目標

未達成目標（請說明，以 100 字為限）

實驗失敗

因故實驗中斷

其他原因

說明：

2. 研究成果在學術期刊發表或申請專利等情形：

論文： 已發表 未發表之文稿 撰寫中 無

專利： 已獲得 申請中 無

技轉： 已技轉 洽談中 無

其他：（以 100 字為限）

3. 請依學術成就、技術創新、社會影響等方面，評估研究成果之學術或應用價值（簡要敘述成果所代表之意義、價值、影響或進一步發展之可能性）（以 500 字為限）

Our studies could be important in the field of quantum information science using quantum dots.